

Optimization of Cs content in Co–Mn–Al mixed oxide as catalyst for N₂O decomposition

Ž. Chromčáková^{1,2} · L. Obalová^{1,2} · P. Kustrowski³ ·
M. Drozdek³ · K. Karásková² · K. Jirátová⁴ ·
F. Kovanda⁵

Received: 27 October 2014 / Accepted: 11 March 2015 / Published online: 18 April 2015
© Springer Science+Business Media Dordrecht 2015

Abstract A series of Co–Mn–Al mixed oxide catalysts with different Cs contents (0.5–4.6 wt%) was prepared by calcination of Co–Mn–Al hydrotalcite (Co:Mn:Al = 4:1:1), followed by impregnation by cesium salt (CsNO₃, Cs₂CO₃) using the pore filling method. Chemical analysis, N₂ sorption, temperature programmed reduction (TPR)-H₂, temperature programmed desorption (TPD)-CO₂ and TPD-NH₃ and X-ray photoelectron spectroscopy (XPS) were used to characterize the catalysts. All prepared catalysts were tested for N₂O catalytic decomposition in inert gas and in the presence of oxygen, water vapor and nitric oxide. The influence of Cs salts used for catalyst preparation and cesium content on catalyst activity were studied. A significant increase in catalytic activity with increasing amount of cesium promoter was observed without respect to the Cs precursor. The strong promotional effect of cesium is electronic in nature and is discussed in term of changes in surface composition and catalyst reducibility.

Keywords Nitrous oxide · Catalytic decomposition · Mixed oxide catalysts · Cesium promoter · Layered double hydroxides

✉ L. Obalová
lucie.obalova@vsb.cz

- ¹ Institute of Environmental Technology, VŠB - Technical University of Ostrava, 17. listopadu 15, 708 33 Ostrava, Czech Republic
- ² Faculty of Metallurgy and Materials Engineering, VŠB - Technical University of Ostrava, 17. listopadu 15, 708 33 Ostrava, Czech Republic
- ³ Jagiellonian University, Ingardena 3, 30-060 Krakow, Poland
- ⁴ Institute of Chemical Process Fundamentals of the ASCR, v.v.i., Rozvojová 135, 165 02 Prague, Czech Republic
- ⁵ University of Chemistry and Technology Prague, Technická 5, 166 28 Prague, Czech Republic

Introduction

Nitrous oxide (N_2O) is known as strong greenhouse gas and it also contributes to depletion of the stratospheric ozone layer. Catalytic decomposition of N_2O to N_2 and O_2 can be an effective method for abatement of N_2O emissions from the chemical industry, especially from nitric acid production plants.

The main problem with the catalysts for N_2O decomposition is that their activity strongly decreases in the presence of oxygen and water vapor, which are the components of waste gas from nitric acid production plants. One of the systems tested by our group achieving high catalytic activity in N_2O decomposition is the Co–Mn–Al mixed oxide with a Co:Mn:Al molar ratio of 4:1:1 [1]. Our effort to increase catalytic activity of the mentioned catalyst led us to study the effect of its modification with low amounts of promoters. Various promoters of catalysts for N_2O decomposition have been reported, namely alkali metals [2–12] or noble metals (Pt, Rh, Pd, Au) [13–15]. We have tested various alkali metals as promoters in Co–Mn–Al mixed oxide catalysts [5–8] and the best results, i.e., the highest N_2O conversions, were achieved over the cesium-promoted samples.

Many factors can affect the catalytic activity of mixed oxide catalyst modified with alkali promoters; for example, the chosen alkali metal promoters and their concentrations [2–5, 7–12], the method of catalyst modification, and the salt used as a promoter precursor [4, 11]. Although the effect of cesium promoters on the activity of catalysts for N_2O decomposition was studied in many reports [2–4, 9, 10, 12], a detailed study of modification of the Co–Mn–Al mixed oxide catalyst with Cs has not yet been published. In this work, the Co–Mn–Al mixed oxides with various contents of Cs promoter were prepared and tested in the catalytic decomposition of N_2O in order to find an optimal promoter concentration. The effect of the Cs salt used for catalyst modification on their catalytic activity was studied as well.

Experimental design

Catalyst preparation and characterization

The Co–Mn–Al mixed oxide with a Co:Mn:Al molar ratio of approximately 4:1:1 was obtained by calcination (500 °C) of Co–Mn–Al layered double hydroxide (LDH) precursor prepared by coprecipitation of the corresponding nitrates; details of the synthesis are described in our former reports [1, 16]. The calcination product was crushed and sieved to obtain a fraction with particle size of 0.160–0.315 mm, which was used in further experiments. The Co–Mn–Al mixed oxide non-modified with Cs promoter was labeled as $\text{Co}_4\text{MnAlO}_x$.

Cesium promoter, in amounts from 0.6 to 4.5 wt% Cs, was loaded on the Co–Mn–Al mixed oxide by the pore filling impregnation method (incipient wetness impregnation). Aqueous solution of cesium salt (CsNO_3 or Cs_2CO_3) of appropriate concentration (corresponding in quantity to the measured total pore volume) was added into a beaker with Co–Mn–Al mixed oxide. The wet samples were dried at

105 °C, calcined for 4 h at 500 °C in air, and then crushed and sieved to obtain a fraction with particle size of 0.160–0.315 mm. Catalysts were labeled according to cesium content and used Cs salt as “nitr” (impregnated by CsNO₃) or “carb” (impregnated by Cs₂CO₃); for example, the 0.6 Cs-nitr sample means the Co–Mn–Al mixed oxide catalyst containing 0.6 wt % Cs modified by impregnation in CsNO₃ solution. A summary of the prepared catalysts is presented in Table 1.

The chemical composition of the prepared catalysts was determined by the atomic absorption spectrometry (AAS) method using a SpectrAA 880 instrument (Varian) after dissolving the samples in hydrochloric acid.

N₂ physisorption on catalyst spheres was performed using a Micromeritics ASAP 2020 instrument after drying at 105 °C under 1 Pa vacuum for 24 h. The adsorption–desorption isotherms of nitrogen at –196 °C were treated by the standard Brunauer–Emmett–Teller (BET) procedure to calculate the specific surface area S_{BET} . The surface area of mesopores S_{meso} and the volume of micropores V_{micro} were determined by the t-plot method. Pore-size distribution (pore radius 10⁰–10² nm) was calculated from the desorption branch of the adsorption–desorption isotherm by the advanced Barrett–Joyner–Halenda (BJH) method [17, 18]. The Lecloux–Pirard standard isotherm [19] was employed for the t-plot as well as for the pore-size distribution evaluation.

Temperature programmed reduction (H₂-TPR) measurements were performed with a sample weight of 0.025 g, a H₂/N₂ mixture (10 mol% H₂), flow rate of 50 ml min^{–1} and linear temperature increase of 20 °C min^{–1} up to 525 °C. A change in H₂ concentration was detected with a mass spectrometer Omnistar 300 (Pfeiffer Vacuum, Germany).

Table 1 Chemical analysis and porous structure of Co–Mn–Al mixed oxide modified with cesium

Sample	Cs (wt %)	Cs salt	Cs/Co molar ratio	S_{BET} (m ² g ^{–1})	V_{meso} (cm ³ g ^{–1})	V_{micro} (mm ³ g ^{–1})
Co ₄ MnAlO _x	0	–	0	92	0.31	21.9
0.6 % Cs-nitr	0.62	NO ₃ [–]	0.013	91	0.19	16.5
1.8 % Cs-nitr	1.82	NO ₃ [–]	0.038	n.d.	n.d.	n.d.
2.0 % Cs-nitr	1.98	NO ₃ [–]	0.042	82	0.18	15.3
2.8 % Cs-nitr	2.76	NO ₃ [–]	0.059	91	0.18	17.1
3.2 % Cs-nitr	3.18	NO ₃ [–]	0.071	100	0.58	20.9
3.4 % Cs-nitr	3.40	NO ₃ [–]	0.069	n.d.	n.d.	n.d.
3.9 % Cs-nitr	3.94	NO ₃ [–]	0.087	n.d.	n.d.	n.d.
4.5 % Cs-nitr	4.51	NO ₃ [–]	0.098	87	0.16	17.7
1.1 % Cs-carb	1.12	CO ₃ ^{2–}	0.024	93	0.17	17.6
1.4 % Cs-carb	1.40	CO ₃ ^{2–}	0.030	66	0.40	14.3
1.9 % Cs-carb	1.85	CO ₃ ^{2–}	0.041	n.d.	n.d.	n.d.
3.6 % Cs-carb	3.55	CO ₃ ^{2–}	0.054	86	0.40	15.7
3.8 % Cs-carb	3.75	CO ₃ ^{2–}	0.080	n.d.	n.d.	n.d.

n.d. not determined

Temperature programmed desorption (TPD) of NH_3 and CO_2 was used to examine acid and basic properties of the catalysts, respectively. The measurements were carried out with a sample weight of 0.05 g in the temperature range of 25–500 °C, with helium as a carrier gas and NH_3 or CO_2 as adsorbing gases. Details of the TPD measurements can be found in [5].

Surface analysis was performed using a Prevac photoelectron spectrometer equipped with a hemispherical VG SCIENTA R3000 analyzer. The $\text{AlK}\alpha$ monochromatized line ($E = 1486.6$ eV) was used for excitation, whereas a low energy electron flood gun (FS40A-PS) compensated for the charge on the surface of nonconductive samples. The binding energies for all samples were referenced to the C 1s core level (284.6 eV) from hydrocarbon contaminations. The surface composition of the samples was evaluated on the basis of the areas and binding energies of Co 2p, Mn 2p, Cs 3d, O 1s, Al 2p and C 1s photoelectron peaks. High resolution spectra were resolved by fitting each peak with a mixed Gaussian–Lorentzian function after a Shirley background subtraction using Casa XPS software.

Catalytic measurements

Catalytic measurements of N_2O decomposition were performed in an integral fixed bed stainless steel reactor of 5 mm internal diameter in the 210–450 °C temperature range under atmospheric pressure. The catalysts bed contained 0.1 g of the sample with a particle size of 0.160–0.315 mm. Total flow was kept at 100 ml min^{-1} ($\text{WHSV} = 60,000 \text{ l h}^{-1} \text{ kg}^{-1}$). The feed introduced to the reactor contained 0.1 mol % N_2O in helium. Oxygen (5 mol%), water vapor (3 mol%) and NO (0.02 mol%) were added to some experimental runs. Prior to each run, the catalysts were treated by heating in He flow at 450 °C and maintaining this temperature for 1 h. After this, N_2O was added to the reaction mixture and the steady state of N_2O concentration level at 450 °C was measured. Then reactor was cooled down to 210 °C with temperature steps of 30 °C. Infrared spectrometers (GMS 810 Series, Sick, Germany and Ultramat 6, Siemens, Germany) and a Fourier transform infrared (FTIR) spectrometer (Nicolet Antaris IGS Analyzer, USA) were used for N_2O and NO analysis. The absolute error of N_2O conversion $X_{\text{N}_2\text{O}}$ (%) evaluated from repeated catalytic runs was $X_{\text{N}_2\text{O}} \pm 4$ (%). The content of the water vapor was determined from measurements of temperature and relative humidity.

Results and discussion

Characterization of the catalysts

Chemical composition of the non-modified $\text{Co}_4\text{MnAlO}_x$ catalyst determined by AAS was 52.0 wt % Co, 10.7 wt % Mn and 5.7 wt % Al; the determined Co:Mn:Al molar ratio of 4:0.88:0.96 corresponded approximately to the value of 4:1:1 adjusted in the nitrate solution used for coprecipitation of the LDH precursor. Eight samples containing 0.6–4.5 wt% Cs were prepared by impregnation of $\text{Co}_4\text{MnAlO}_x$ sample

with CsNO_3 aqueous solution and five samples containing 1.1–3.8 wt% Cs were prepared by impregnation with Cs_2CO_3 aqueous solution. Cesium contents in the prepared catalysts are summarized in Table 1, together with results of surface area measurements and porous structure analysis. Surface areas of the samples modified with Cs were similar compared to the parent Co–Mn–Al mixed oxide and varied around $90 \text{ m}^2 \text{ g}^{-1}$. Lower surface area ($66 \text{ m}^2 \text{ g}^{-1}$) determined for the 1.4 % Cs-carb catalyst was probably connected with lower volume of micropores. Three samples (3.2 % Cs-nitr, 1.4 % Cs-carb and 3.6 % Cs-carb) exhibited substantially higher mesopore volumes than the other catalysts.

The TPR profiles of Co–Mn–Al mixed oxides modified with various amounts of cesium are shown in Fig. 1. As the measurements of N_2O decomposition were performed up to $450 \text{ }^\circ\text{C}$, only the species reduced in the temperature range from 25 to $500 \text{ }^\circ\text{C}$ were considered to be involved in the catalytic reaction. The hydrogen consumptions and temperatures of reduction maxima are presented in Table 2. It is obvious that the presence of cesium influenced the reducibility of catalysts; reduction of Co^{3+} to Co^{2+} , considered as the rate-determining step of N_2O decomposition, was facilitated.

The amounts of surface acidic and basic sites as determined by temperature programmed desorption of NH_3 and CO_2 are presented in Table 2. The non-modified $\text{Co}_4\text{MnAlO}_x$ catalyst was the most acidic and showed the lowest basicity. Increasing cesium content in the catalysts suppressed acidity and increased basicity; the amount of desorbed NH_3 decreased from 0.50 to 0.24 mmol g^{-1} and the amount of desorbed CO_2 increased from 0.16 to 0.32 mmol g^{-1} , as was determined for the non-modified $\text{Co}_4\text{MnAlO}_x$ sample and 4.5 % Cs-nitr sample with the highest Cs content, respectively.

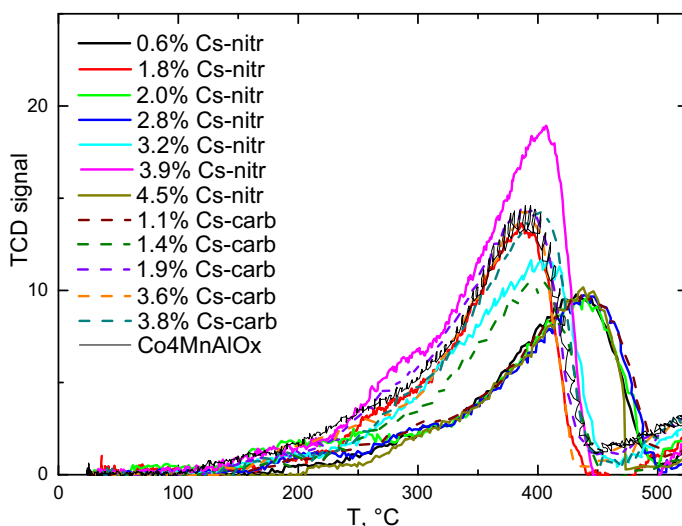


Fig. 1 H_2 -TPR profiles of Co–Mn–Al mixed oxides modified with cesium

Table 2 TPR-H₂, TPD-CO₂ and TPD-NH₃ of Co–Mn–Al mixed oxides modified with cesium

Sample	TPR-H ₂ mmol/g (25–500 °C)	T _{max} (°C)	NH ₃ -TPD mmol/g (25–500 °C)	CO ₂ -TPD mmol/g (25–500 °C)
Co ₄ MnAlO _x ^a	4.01	391 (401)	0.50	0.16
0.6 Cs-nitr	3.84	432	0.39	0.28
1.8 Cs-nitr	3.56	388	n.d.	n.d.
2.0 Cs-nitr	4.40	436	0.19	0.22
2.8 Cs-nitr	4.14	440	0.35	0.18
3.2 Cs-nitr	4.22	402	0.32	0.23
3.4 Cs-nitr	3.49	407	n.d.	n.d.
3.9 Cs-nitr	5.09 (5.15)	406	n.d.	n.d.
4.5 Cs-nitr	3.56	438	0.24	0.32
1.1 Cs-carb	4.20	440	0.45	0.27
1.4 Cs-carb	3.40	405	0.20	0.19
1.9 Cs-carb	4.55	392	n.d.	n.d.
3.6 Cs-carb	3.44	389	0.19	n.d.
3.8 Cs-carb	4.25 (4.46)	402	n.d.	n.d.

^a Data from [17]

The XPS data (Table 3) provide information about the content and chemical state of the elements in the surface layer of the sample. We suppose that cesium is located mainly on the surface, as it was introduced by impregnation of the parent mixed oxide catalyst. The binding energy for the Cs 3d_{5/2} was determined as 724.2 ± 0.2 eV. Co is located on the surface in two chemical states, namely as Co²⁺ with a lower binding energy of 779.8 ± 0.2 eV and Co³⁺ with a higher binding energy of 781.5 ± 0.1 eV. Two chemical states of manganese were also identified in all cesium-modified samples: Mn³⁺ with a lower binding energy of 641.5 ± 0.5 eV and Mn⁴⁺ with a higher binding energy of 643.2 ± 0.3 eV. Oxygen is present on the surface of all samples in several chemical states, (data not shown) – mainly as O²⁻ lattice ions, but also in the form of hydroxyls, strongly adsorbed water and/or carbonates.

Table 3 Binding energies of core level electrons and surface chemical composition, as determined from XPS

Catalyst	Cs 3d _{5/2}	Co 2p _{3/2}	$\frac{\text{Co}^{2+}}{\text{Co}^{3+}}$	Mn 2p _{3/2}	Co:Mn:Al	$\frac{\text{Cs}}{\text{Co}}$	$\frac{\text{Cs}}{(\text{Co} + \text{Mn} + \text{Al})}$		
Co ₄ MnAlO _x ^a	–	780.0	781.7	2.34	641.3	643.0	4:1.0:2.0	–	–
1.8 % Cs-nitr	724.3	780.1	781.5	1.09	641.7	643.5	4:0.9:1.81	0.097	0.058
3.9 % Cs-nitr	724.0	779.7	781.4	2.07	641.4	643.1	4:1:2.04	0.190	0.108
1.9 % Cs-carb	724.2	779.8	781.5	1.49	641.5	643.3	4:1:1.67	0.099	0.059
3.8 % Cs-carb	724.2	779.8	781.5	1.77	641.4	643.0	4:1:1.72	0.233	0.138

^a Data from [20]

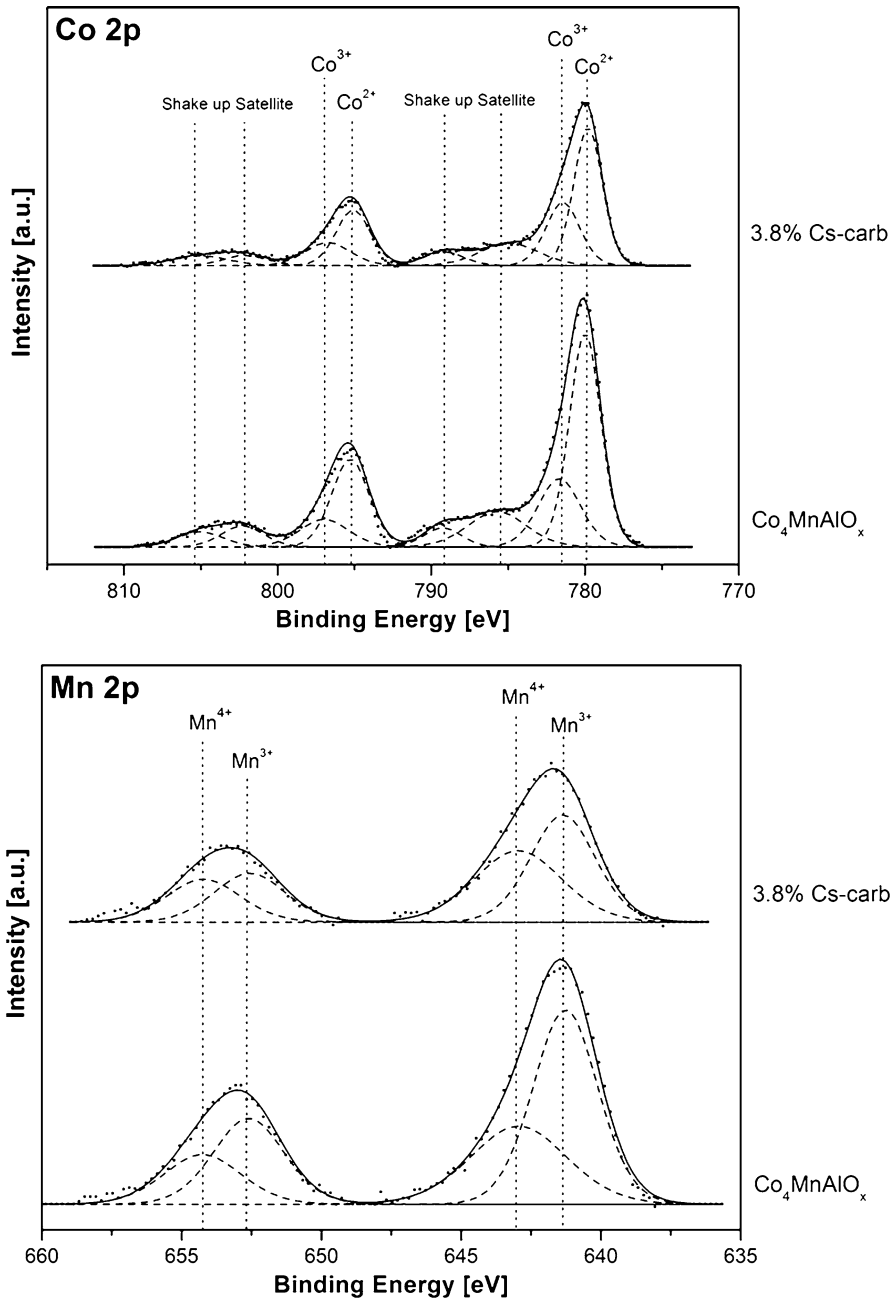


Fig. 2 XPS spectra of Co 2p and Mn 2p electrons over Co–Mn–Al mixed oxide catalysts modified with cesium promoter

Due to electron donation from an alkali metal to a transition metal, a decrease in the work function and shift to a lower binding energy can be expected [9]. Indeed, after the modification of Co–Mn–Al mixed oxide with cesium, a shift of the Co $2p_{3/2}$ peak to the slightly lower values of binding energy was observed (Fig. 2). Furthermore, an evident decrease in the $\text{Co}^{2+}/\text{Co}^{3+}$ molar ratio was found after catalyst modification with Cs, and the $\text{Co}^{2+}/\text{Co}^{3+}$ molar ratio increased with increasing cesium content.

N_2O catalytic decomposition

Co–Mn–Al mixed oxides modified with cesium promoter were tested in the catalytic decomposition of N_2O ; the effects of Cs content and Cs salt used for catalysts impregnation on activity of the examined catalysts were studied. The temperature dependencies of N_2O conversion in inert gas are shown in Fig. 3. Modification of the parent Co–Mn–Al mixed oxide catalysts with cesium promoter significantly changed its catalytic activity. Nearly the same N_2O conversions were reached over the catalysts modified with the similar promoter amounts, independently of the used solutions of Cs salt. The N_2O conversion increased with increasing Cs content in the catalysts in the studied Cs concentration range (Fig. 4). N_2O was selectively decomposed to N_2 and O_2 and no other nitrogen containing products were detected by FTIR method. An internal diffusion limitation of the

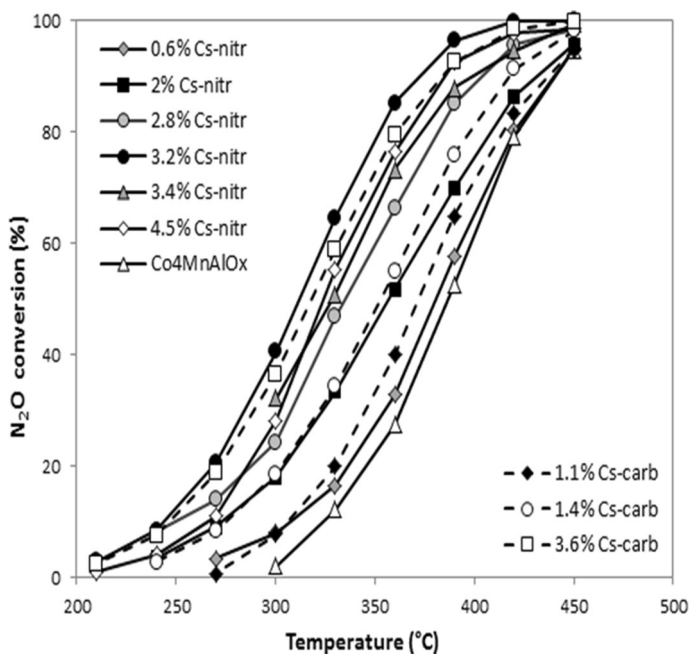


Fig. 3 Temperature dependence of N_2O conversion over Co–Mn–Al mixed oxide catalysts modified with cesium promoter. Conditions: 0.1 mol% N_2O in He, $\text{SV} = 60 \text{ lg}^{-1} \text{ h}^{-1}$

reaction rate is expected at higher temperatures according to results of our previous work [21]. The maximal hindering of the reaction rate by diffusion in pores expressed as an internal effectiveness factor was 0.92 at 450 °C.

The N_2O catalytic decomposition over alkali promoted Co–Mn–Al mixed oxides proceeds via a cationic redox mechanism when transition metal ions act as donor centers of surface electrons, stimulating the transfer of electron density for activation of the N_2O molecule, and further as electron acceptor centers for the resultant surface O^- intermediates [20]. According to reported studies [2, 20, 22–24], mechanism of the N_2O catalytic decomposition can be described as a charge donation from the catalyst to the anti-bonding orbital of N_2O , which destabilizes the N–O bond, leading to scission. Therefore, electron charge transfer from the metal ion to the N_2O molecule is a crucial step for N_2O catalytic decomposition [24]. The reduction of the metal ion to a low oxidation state is a subsequent, very important step for the regeneration of the active centers [20].

The studied mixed oxide catalysts could be applied in abatement of N_2O emissions from nitric acid production plants. Therefore, it is necessary to examine the effect of other gases present in the reaction mixture (namely O_2 , H_2O and NO) on the catalysts activity and stability.

The effect of oxygen and water vapor added to the inlet gas on the activity of Co–Mn–Al mixed oxides modified with similar amounts of cesium is shown in Fig. 5. The same N_2O conversions were observed over the catalysts with nearly the same Cs contents; the Cs salt used for the mixed oxide modification had no effect. Compared to N_2O conversions measured in the inert gas (Fig. 3), the presence of O_2

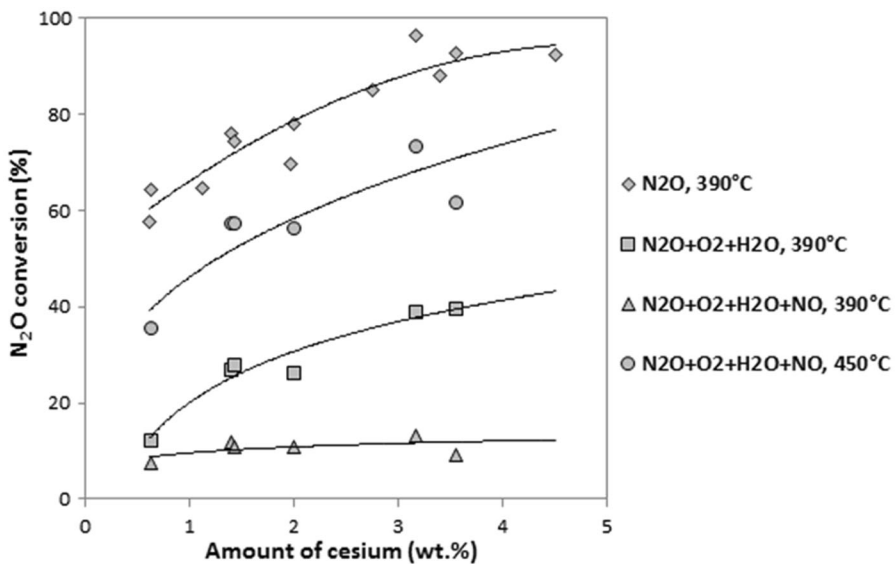


Fig. 4 Dependence of N_2O conversion on the content of cesium promoter in Co–Mn–Al mixed oxide catalysts. Conditions: 0.1 mol% N_2O , 5 mol% O_2 , 3 mol% H_2O , 0.02 mol% NO in He, $\text{SV} = 60 \text{ lg}^{-1} \text{ h}^{-1}$

and H_2O in the reaction mixture had an inhibiting effect and caused a decrease in catalytic activity due to their accumulation on the catalysts surface. The N_2O conversion at 450°C decreased about 10 % over the catalysts with higher Cs content (above 3 wt% Cs), whereas a decrease of about 30–60 % in N_2O conversion was observed over the catalysts with lower Cs loading (under 2 wt% Cs). According to the results of N_2O -TPD tests reported by Pasha et al. [9], the presence of higher amount of Cs in the Co catalysts (molar ratio Cs/Co above 0.05) causes weakening of Co–O bond and early release of oxygen from the catalyst surface. A similar trend with desorbing of water vapor was also observed; the H_2O -TPD experiments showed early release of water vapor over the catalyst with the higher cesium content in comparison with the parent bulk catalyst. Our results were in agreement with these findings.

In the presence of oxygen, water vapor and NO (Fig. 6), no differences in N_2O conversion were observed over the catalysts prepared by impregnation with Cs_2CO_3 and CsNO_3 solutions. A shift of conversion curves to the higher temperatures compared to the experiment in the reaction mixture containing only $\text{O}_2 + \text{H}_2\text{O}$ was observed for all catalysts. In case of measurements in the presence of inhibiting gases (O_2 , H_2O and NO), it was found that added NO was oxidized to NO_2 .

During N_2O catalytic decomposition in the presence of NO, a decrease in NO concentration was also observed when NO conversion increased with decreasing temperature (Fig. 7); the cesium content in the catalysts as well as Cs salt used for impregnation had no effect.

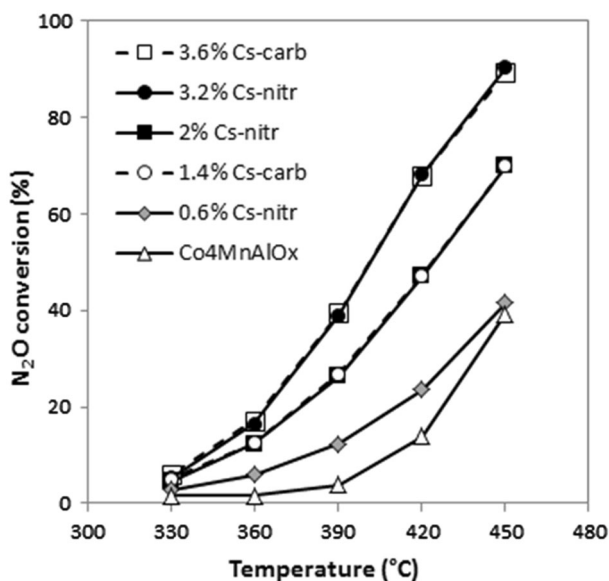


Fig. 5 Temperature dependence of N_2O conversion in presence of O_2 and H_2O over Co–Mn–Al mixed oxide catalysts modified with cesium promoter. Conditions: 0.1 mol% N_2O , 5 mol% O_2 , 3 mol% H_2O in He, SV = $60 \text{ lg}^{-1} \text{ h}^{-1}$

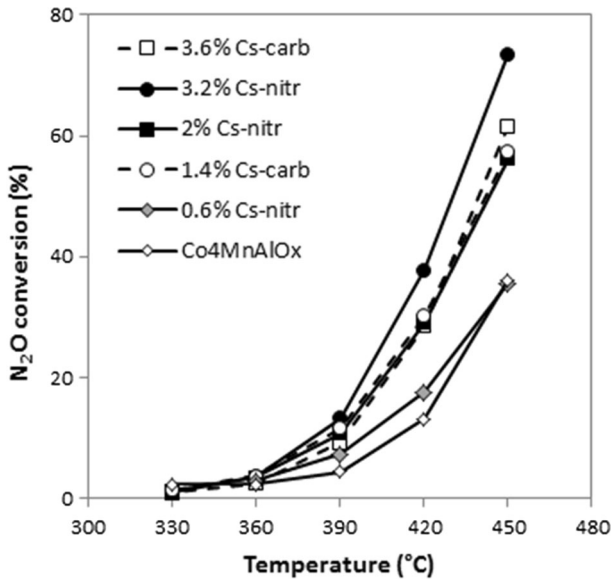


Fig. 6 Temperature dependence of N₂O conversion in presence of O₂, H₂O and NO over Co–Mn–Al mixed oxide catalysts modified with cesium promoter. Conditions: 0.1 mol% N₂O, 5 mol% O₂, 3 mol% H₂O, 0.02 mol% NO in He, SV = 60 lg⁻¹ h⁻¹

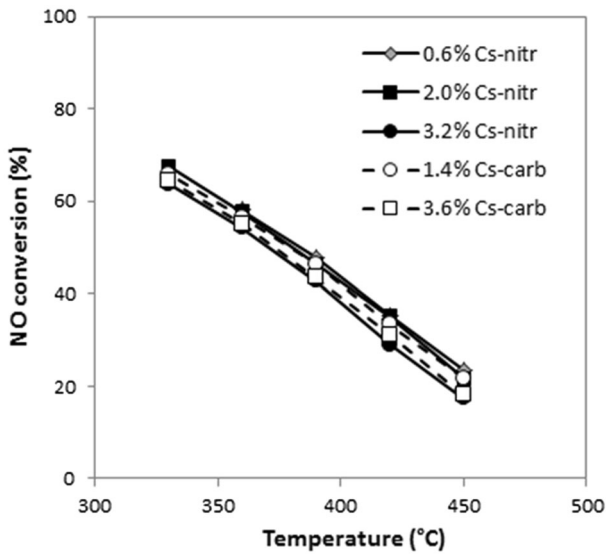


Fig. 7 Temperature dependence of NO conversion in presence of O₂, H₂O and NO over Co–Mn–Al mixed oxide catalysts modified with cesium promoter. Conditions: 0.1 mol% N₂O, 5 mol% O₂, 3 mol% H₂O, 0.02 mol% NO in He, SV = 60 lg⁻¹ h⁻¹

Dependence of N_2O conversion on the content of cesium promoter in Co–Mn–Al mixed oxide catalysts and composition of the reaction mixture is shown in Fig. 4. The N_2O conversion increased with increasing Cs content in all tested reaction mixtures, although in the case of N_2O conversion in inert, optimal Cs loading seems to appear around 3–4.5 wt% Cs and the decrease in catalytic activity with further addition of cesium could be expected. Taking into account the results reported by Pasha et al. [12], this effect can be ascribed to a decrease in number of available sites active in N_2O decomposition.

As we recently reported [20], modification of Co–Mn–Al mixed oxide catalysts with alkali metals, especially with cesium, resulted in changing reducibility of the catalysts. The results presented herein show the increase in N_2O conversions with decreasing temperatures of reduction maxima measured with the examined catalysts with different content of Cs (Fig. 8). The shift of T_{max} to the lower temperatures observed with increasing content of Cs in catalysts can be explained by easier reduction of Co^{3+} and Mn^{4+} corresponding to the weakening of their bonds with oxygen, which facilitates desorption of oxygen from the catalyst surface [20]. Observed changes in catalyst reducibility are in agreement with results of XPS and changes in the $\text{Co}^{2+}/\text{Co}^{3+}$ molar ratio, since not only easy reduction of Co^{3+} but also easy oxidation of Co^{2+} in the course of electron donation to the N_2O molecule is important for the high reaction rate of N_2O decomposition [10, 11, 24, 25].

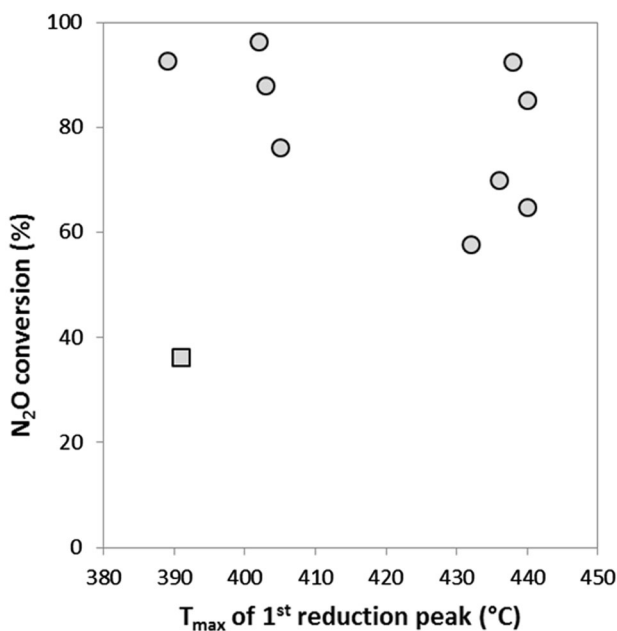


Fig. 8 Dependence of catalytic activity on T_{max} of H_2 -TPR reduction peak of Co–Mn–Al mixed oxides modified with cesium. Conditions: 0.1 mol% N_2O in He, 390 °C, SV = 60 $\text{lg}^{-1} \text{h}^{-1}$

Conclusions

The N₂O catalytic decomposition over Co–Mn–Al mixed oxides promoted with various amounts of cesium was examined in an inert gas and in the presence of oxygen, water vapor and nitric oxide. The cesium promoter was added by impregnation with an aqueous solution of two different Cs salts, namely CsNO₃ and Cs₂CO₃. The kind of Cs salts used had no effect on chemical properties, porous structure or catalytic activity of the prepared catalysts. The catalytic activity in N₂O decomposition increased with increasing content of cesium promoter, which was connected with observed changes in catalyst reducibility and the Co²⁺/Co³⁺ surface molar ratio, as the effect of the Cs promoter is of electronic origin. The catalysts with high promoter contents of about 3.2–4.5 wt % Cs showed the highest activity in the presence of other gases (NO, O₂, H₂O) that occur in the waste gas upstream of the selective catalytic reduction of NO_x (SCR NO_x) unit in nitric acid production plants.

Acknowledgments This work was supported by the Czech Science Foundation (Project No. 14-13750S) and by the Ministry of Education, Youth and Sports of the Czech Republic in the “National Feasibility Program I,” project LO1208 “Theoretical Aspects of Energetic Treatment of Waste and Environment Protection against Negative Impacts” and by the specific research projects SP2014/48, SP2014/62 and SP2015/125.

References

1. L. Obalová, K. Jiráťová, F. Kovanda, K. Pacultová, Z. Lacný, Z. Mikulová, *Appl. Catal. B* **60**, 289–297 (2005)
2. B.M. Abu-Zied, *Chin. J. Catal.* **32**, 264–272 (2011)
3. H. Wu, W. Li, L. Guo, Y. Pan, X. Xu, *J. Fuel Chem. Technol.* **39**, 550–555 (2011)
4. Y. Pan, M. Feng, X. Cui, X. Xu, *J. Fuel Chem. Technol.* **40**, 601–607 (2012)
5. L. Obalová, K. Karásková, K. Jiráťová, F. Kovanda, *Appl. Catal. B Environ.* **90**, 132–140 (2009)
6. L. Obalová, G. Maniak, K. Karásková, F. Kovanda, A. Kotarba, *Catal. Commun.* **12**, 1055–1058 (2011)
7. K. Karásková, L. Obalová, K. Jiráťová, F. Kovanda, *Chem. Eng. J.* **160**, 480–487 (2010)
8. K. Karásková, L. Obalová, F. Kovanda, *Catal. Today* **176**, 208–211 (2011)
9. N. Pasha, N. Lingaiah, N. Seshu Babu, P. Siva Sankar Reddy, P.S. Sai Prasad, *Catal. Commun.* **10**, 132–136 (2008)
10. P. Stelmachowski, G. Maniak, A. Kotarba, Z. Sojka, *Catal. Commun.* **10**, 1062–1065 (2009)
11. F. Zasada, P. Stelmachowski, G. Maniak, J.-F. Paul, A. Kotarba, Z. Sojka, *Catal. Lett.* **127**, 126–131 (2009)
12. N. Pasha, N. Lingaiah, P. Siva Sankar Reddy, P.S. Sai Prasad, *Catal. Lett.* **118**, 64–68 (2007)
13. X. Xu, X. Xu, G. Zhang, X. Niu, *J. Fuel Chem. Technol.* **37**, 595–600 (2009)
14. H. Beyer, J. Emmerich, K. Chatziapostolou, K. Köhler, *Appl. Catal. A: Gen* **391**, 411–416 (2011)
15. S. Parres-Esclapez, M.J. Illián-Gómez, C. Salinas-Martínez De Lecea, A. Bueno-López, *Appl. Catal. B Environ.* **96**, 370–378 (2010)
16. F. Kovanda, T. Rojka, J. Dobešová, V. Machovič, P. Bezdička, L. Obalová, K. Jiráťová, T. Grygar, *J. Solid State Chem.* **179**, 812–823 (2006)
17. K.S.W. Sing, R.T. Williams, *Adsorpt. Sci. Technol.* **22**, 773–782 (2004)
18. L. Matějová, O. Šolcová, P. Schneider, *Microporous Mesoporous Mater.* **107**, 227–232 (2008)
19. A. Lecloux, J.P. Pirard, *J. Colloid Interf. Sci.* **70**, 265–281 (1979)
20. L. Obalová, K. Karásková, A. Wach, P. Kustrowski, K. Mamulová-Kutlákova, S. Michalik, K. Jiráťová, *Appl. Catal. A* **462–463**, 227–235 (2013)
21. L. Obalová, K. Jiráťová, K. Karásková, Ž. Chromčáková, *Catal. Today* **191**, 116–120 (2012)

22. Z. Dou, M. Feng, X. Xu, J. Fuel Chem. Technol. **41**, 1234–1240 (2013)
23. B.M. Abu-Zied, S.A. Soliman, Catal. Lett. **132**, 299–310 (2009)
24. G. Maniak, P. Stelmachowski, F. Zasada, W. Piskorz, A. Kotarba, Z. Sojka, Catal. Today **176**, 369–372 (2011)
25. P. Stelmachowski, G. Maniak, J. Kaczmarczyk, F. Zasada, W. Piskorz, A. Kotarba, Z. Sojka, Appl. Catal. B Environ. **146**, 105–111 (2014)